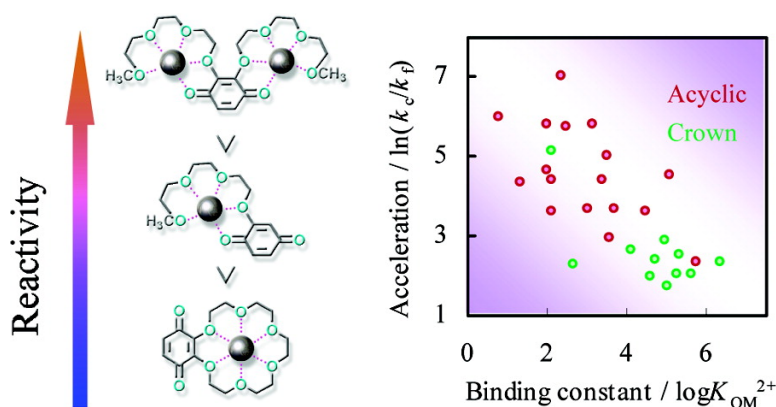Article

Self-Activated Supramolecular Reactions: Effects of Host–Guest Recognition on the Kinetics of the Diels–Alder Reaction of Open-Chain Oligoether Quinones with Cyclopentadiene

Akihiko Tsuda, Chikako Fukumoto, and Takumi Oshima

More About This Article

Additional resources and features associated with this article are available within the HTML version:

- Supporting Information
- Access to high resolution figures
- Links to articles and content related to this article
- Copyright permission to reproduce figures and/or text from this article

View the Full Text HTML

Self-Activated Supramolecular Reactions: Effects of Host−Guest Recognition on the Kinetics of the Diels−Alder Reaction of Open-Chain Oligoether Quinones with Cyclopentadiene

Akihiko Tsuda,*,† Chikako Fukumoto, and Takumi Oshima*

Contribution from the Department of Materials Chemistry, Graduate School of Engineering, Osaka University, Toyonaka, Osaka 560-0043, Japan

Received December 13, 2002; E-mail: tsuda@macro.t.u-tokyo.ac.jp; oshima@ch.wani.osaka-u.ac.jp

Abstract: Diels−Alder reactions of acyclic oligoether-substituted quinones **1b**, **1c**, **2b**, and **2c** with cyclopentadiene were accelerated by the addition of alkali and alkaline earth metal perchlorates, and scandium trifluoromethane sulfonate (k_c/k_f = 1.2−23 for univalent cations, 11−1160 for divalent cations, and 1700−192 000 for Sc^{3+}, where k_c and k_f are the rate constants for the metal complexed and uncomplexed quinones, respectively). The shorter-armed **1a**, **2a**, and **3**, however, exhibited no such acceleration effects. The rate accelerations can be rationalized by the FMO consequence in which the bound guest cation withdraws electron density from the quinone dienophile and lowers the LUMO energy suitable for the orbital interaction with the HOMO of cyclopentadiene. Despite the poor cation selectivity, these acyclic oligoether quinones showed larger rate accelerations than the relevant quinocrown ethers **4** (k_c/k_f = 1.3−3.0 for univalent cations, 5.0−160 for divalent cations, and 100−2020 for Sc^{3+}). The effective electron withdrawal, which leads to the enhanced rate acceleration, can be caused by the direct interaction between the metal cation accommodated in the pseudo-cyclic oligoether linkage and the quinone carbonyl oxygen, as indicated by ^{1}H NMR spectroscopy. In addition, the larger rate enhancement is rather achieved in the complex with low binding constant *K*, because the strong encapsulation of metal cation by the oligoether chain diminishes the crucial interaction to the quinone carbonyl oxygen. As a whole, the smaller and higher valent cations tend to bring about notable rate acceleration due to the more enhanced ion−dipole interaction with the quinone carbonyl oxygen. Spectroscopic titration (absorption and ^{1}H NMR) and kinetic experiments indicated that only the longest di-armed **2c** constructs 1:1, and then 1:2, host/guest complexes with Ca^{2+}, Sr^{2+}, and Ba^{2+}. These 1:2 complexes exhibited the most effective acceleration for the respective metal cations.

Introduction

Catalysis of organic reactions by supramolecules is a current research interest in supramolecular chemistry.[1] These catalytic reactions can be divided into about three categories as represented in Scheme 1. The guest-activation by molecular recognition, in which the electronic properties and environment of the guest reactant are altered by complexation, brings about acceleration of the reactions (A).[2] The close-packing by accommodation of both reactants into the space or cavity of the

supramolecules also enhances their reactivity due to the close location and independence from external environments (B).[3] However, little is known about "self-activation" of host molecules by incorporation of the guest (C).[4,5]

In organisms, it is well known that metal ion recognition by proteins plays an important role as a trigger of reactions related with many biological phenomena.[6] In those systems, proteins
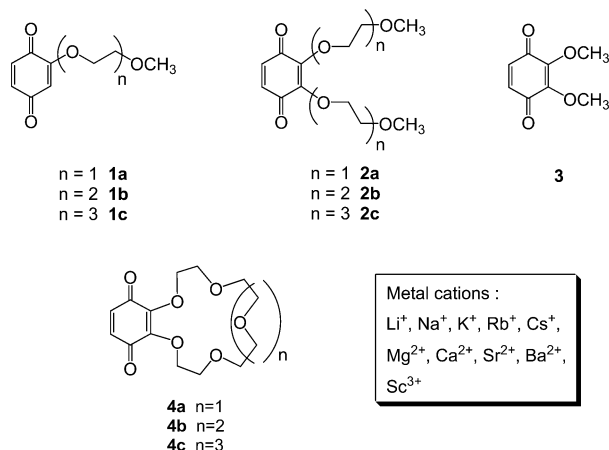
† Present address: Department of Chemistry and Biotechnology, School of Engineering, The University of Tokyo, 7-3-1 Hongo, Bunkyo-ku, Tokyo 113-8656, Japan.

(1) Lehn, J.-M. *Supramolecular Chemistry*; VCH: Weinheim, Germany, 1995.

(2) (a) Hosseini, M. W.; Lehn, J.-M. *J. Am. Chem. Soc.* **1987**, *109*, 7047. (b) Diederich, F.; Lutter, H.-D. *J. Am. Chem. Soc.* **1989**, *111*, 8438. (c) Gobbi, A.; Landini, D.; Maria, A.; Penso, M. *J. Chem. Soc., Perkin Trans. 2* **1996**, 2505. (d) Mattei, P.; Diederich, F. *Helv. Chim. Acta* **1997**, *80*, 1555. (e) Cacciapaglia, R.; Mandolini, L.; Arnecke, R.; Böhmer, V.; Vogt, W. *J. Chem. Soc., Perkin Trans. 2* **1998**, 419. (f) Brrecia, P.; Cacciapaglia, R.; Mandolini, L.; Scorsini, C. *J. Chem. Soc., Perkin Trans. 2* **1998**, 1257. (g) Reetz, M. T.; Waldvogel, S. R. *Angew. Chem., Int. Ed. Engl.* **1997**, *36*, 865. (h) Castelli, V. v. A.; Cort, A. D.; Mandolini, L. *J. Am. Chem. Soc.* **1998**, *120*, 12688. (i) Merlau, M. L.; Mejia, M. d. P.; Nguyen, S. T.; Hupp, J. T. *Angew. Chem., Int. Ed.* **2001**, *40*, 4239.

(3) (a) Kang, J.; Rebek, J., Jr. *Nature* **1997**, *385*, 50. (b) Endo, K.; Koike, T.; Sawaki, T.; Hayashida, O.; Masuda, H.; Aoyama, Y. *J. Am. Chem. Soc.* **1997**, *119*, 4117. (c) Kang, J.; Santamaria, J.; Hilmersson, G.; Rebek, J., Jr. *J. Am. Chem. Soc.* **1998**, *120*, 3650. (d) Kang, J.; Santamaria, J.; Hilmersson, G.; Rebek, J., Jr. *J. Am. Chem. Soc.* **1998**, *120*, 7389. (e) Clyde-Watson, A.; Vidal-Ferran, A.; Twyman, L. J.; Walter, C. J.; McCallien, D. W. J.; Fanni, S.; Bampos, N.; Wilie, R. S.; Sanders, J. K. L. *New J. Chem.* **1998**, *22*, 493. (f) Bassani, D. M.; Darcos, V.; Mahony, S.; Desvergne, J.-P. *J. Am. Chem. Soc.* **2000**, *122*, 8795. (g) Yoshizawa, M.; Takeyama, Y.; Kusukawa, T.; Fujita, M. *Angew. Chem., Int. Ed.* **2002**, *41*, 1347.

(4) (a) Inoue, Y.; Ouchi, M.; Hayama, H.; Hakushi, T. *Chem. Lett.* **1983**, 431. (b) Cacciapaglia, R.; Lucente, S.; Mandolini, L.; Doorn, A. R.; Reinhoudt, D. N.; Verboom, W. *Tetrahedron* **1989**, *45*, 5293. (c) Cacciapaglia, R.; Doom, A. R.; Mandolina, L.; Reinhoudt, D. N.; Verboon, W. *J. Am. Chem. Soc.* **1992**, *114*, 2611. (d) Itoh, S.; Taniguchi, M.; Takada, N.; Nagatomo, S.; Kitagawa, T.; Fukuzumi, S. *J. Am. Chem. Soc.* **2000**, *122*, 12087.

(5) (a) Tsuda, A.; Oshima, T. *New J. Chem.* **1998**, 1027. (b) Tsuda, A.; Oshima, T. *J. Org. Chem.* **2002**, *67*, 1282.

(6) Borle, A. B. *Rev. Physiol. Biochem. Pharmacol.* **1990**, *90*, 13.

Scheme 1. Schematic Representations of Supramolecular Catalytic Reactions[a]
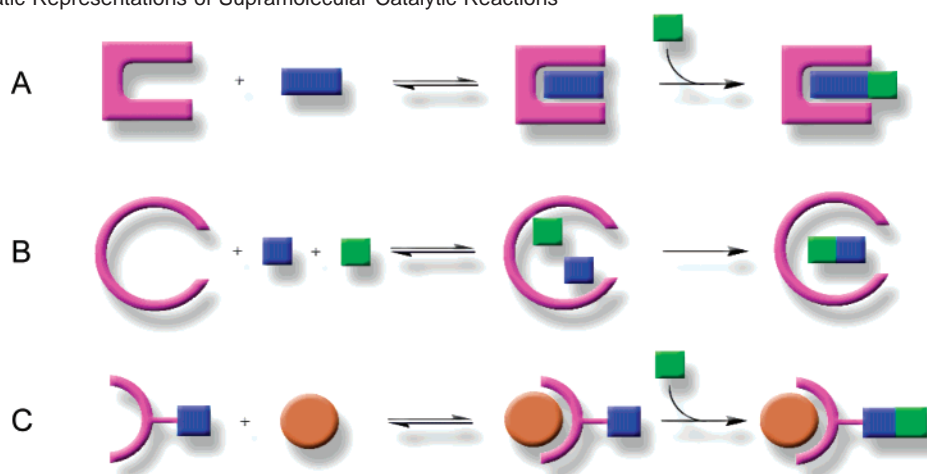
[a] (A) Guest-activation catalysis, (B) close-packing catalysis, and (C) host-activation catalysis.

Chart 1. Acyclic Oligoether Quinones **1**, **2**, Reference **3**, Quinocrown Ethers **4**, and Metal Cations Used in this Study

n = 1 **1a**
n = 2 **1b**
n = 3 **1c**

n = 1 **2a**
n = 2 **2b**
n = 3 **2c**

3

4a n=1
4b n=2
4c n=3

Metal cations :
Li^{+}, Na^{+}, K^{+}, Rb^{+}, Cs^{+},
Mg^{2+}, Ca^{2+}, Sr^{2+}, Ba^{2+},
Sc[3+]

Figure 1. Schematic representation of (a) a helical complex and (b) S-shaped dinuclear complexes.

recognize the appropriate metal cations of peculiar size, valence, stiffness, and concentration to start certain reactions programmed for the respective combinations. The metal cations, therefore, act as a signal material for the information transfer in biological systems. Hence, construction of artificial self-activation models, which mimic such biological systems, will become one way to explore the complicated reaction systems in nature.

We previously reported the effects of host−guest recognition on the kinetics of the Diels−Alder (DA) reaction of quinone crown ethers **4** with cyclopentadiene, in which cation binding of the quinocrown ethers caused large rate accelerations especially in the size-favorable combinations.[5] The principle of the rate acceleration of DA reactions can be readily rationalized by assuming that the incorporated guest cation behaves as an electron-withdrawing group for the quinone dienophile, thus lowering its LUMO energy against the HOMO of cyclopentadiene.[7] In that study, we have found that the magnitude of acceleration is mainly determined by the following three factors. (1) Complex formation stability (binding constant $K_{QM^{m+}}$): the concentration of the complex affects the magnitude of rate enhancement. (2) Coordination geometry of the complex: the
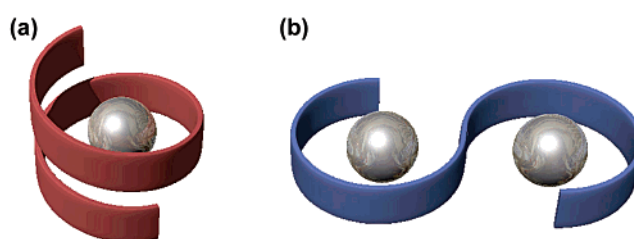
extent of interaction between the incorporated guest cation and oxygen atoms attached at the 2,3-positions of quinone governs the magnitude of rate acceleration. Thus, the complex structure that can enforce close location between the ring-bound cation and those oxygens is highly effective in causing large electron withdrawal from the quinone moiety. Hence, the size-fitted complexes, which may always keep a close distance between the cation and the quinone, can bring about larger acceleration than other size-mismatched complexes. (3) Valency of the cation: the increase of Lewis acidity with increasing valency of the cation leads to the significant rate enhancement.

These interesting findings prompted us to extend the cation-recognized DA reactions to acyclic mono-armed and di-armed oligoether quinones **1** and **2** (Chart 1), because the oligoether chain can accommodate the metal cations with characteristic pseudo-cyclic "helical" conformations, whose structure may lead to effective separation of the incorporated metal cation from its counteranions and/or solvent molecules (Figure 1a).[8,9] As another interesting behavior, the long oligoether chains can construct multinuclear complexes such as 1:2 ligand/metal complexes with S-shaped manner (Figure 1b).[10−12] Their intrinsic flexibilities have bestowed some promising unpredict-

(7) (a) Woodward, R. B.; Hoffmann, R. *Angew. Chem.* **1969**, *81*, 797. (b) Fleming, I. *Frontier Orbitals and Organic Chemical Reactions*; John Wiley: London, 1976.

(8) (a) Vögtle, F.; Weber, E. *Angew. Chem., Int. Ed. Engl.* **1979**, *18*, 753. (b) Saenger, W.; Brand, H. *Acta Crystallogr., Sect. B* **1979**, *35*, 838. (c) Weber, G.; Saenger, W.; Vögtle, F.; Sieger, H. *Angew. Chem., Int. Ed. Engl.* **1979**, *18*, 226.

(9) (a) Suzuki, Y.; Morozumi, T.; Nakamura, H.; Shimomura, S.; Bartsh, R. A. *J. Phys. Chem. B* **1998**, *102*, 7910. (b) Morozumi, T.; Anada, T.; Nakamura, H. *J. Phys. Chem. B* **2001**, *105*, 2923.

(10) Iwamoto, R. *Bull. Chem. Soc. Jpn.* **1973**, *46*, 1114.

(11) Weber, G.; Saenger, W. *Angew. Chem.* **1979**, *91*, 237; *Angew. Chem., Int. Ed. Engl.* **1979**, *18*, 227.

(12) Arunasalam, V.-C.; Baxter, I.; Drake, S. R.; Hursthouse, M. B.; Malik, K. M. A.; Miller, S. A. S.; Mingos, D. M. P.; Otway, D. J. *J. Chem. Soc., Dalton Trans.* **1997**, 1331.

able structures on the complexation with metal cations. However, they have displayed weak affinities with guest cations in comparison with crown ethers.[13] The conformational entropy change for complexation is more favorable for the cyclic ligands, because their donor oxygens are preorganized to interact with a guest species, whereas the acyclic ligands must lose significant freedom to adopt a favorable cyclic conformation for guest binding. With these backgrounds, the quinones bearing an oligoether chain were expected to show interesting behavior for the rate enhancement of the DA reactions by reflecting their unique cation complexation properties.

Herein, we present a systematic study of the effects of cation recognition on the kinetics of DA reactions of open-chain oligoether quinones bearing one oligoether sidearm, **1**, and two oligoether sidearms, **2**, with cyclopentadiene in comparison with the reactions of 2,3-dimethoxy-1,4-benzoquinone, **3**, as a reference compound and quinocrown ethers, **4**, reported previously (Chart 1 and Scheme 2).[14] The guest cations used in this study were univalent Li^+, Na^+, K^+, Rb^+, Cs^+, divalent Mg^{2+}, Ca^{2+}, Sr^{2+}, Ba^{2+}, and trivalent Sc^{3+}.

Scheme 2. Diels−Alder Reaction of the **2c**·M^{m+} Complex with Cyclopentadiene
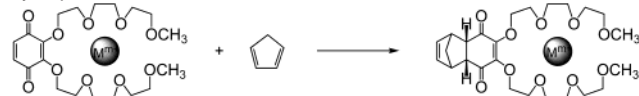
Results and Discussion

Complex Formation between Acyclic Oligoether Quinone and Cation. 1:1 Host−Guest Complexation. The DA reactions in the presence of a metal ion, in which the acyclic host and cation are supposed to form a complex with 1:1 stoichiometry, are to be considered as the following eqs 1−3. In eq 1, the metal ion is able to form a 1:1 complex with the acyclic oligoether quinone Q, where reaction 1 is at rapid equilibrium with its binding constant K_{QM}^{m+}.

$$Q \quad + \quad M^{m+} \quad \rightleftharpoons \quad QM^{m+} \qquad (1)$$

$$\alpha[Q]_t \qquad [M^{m+}]_t - (1-\alpha)[Q]_t \qquad (1-\alpha)[Q]_t$$
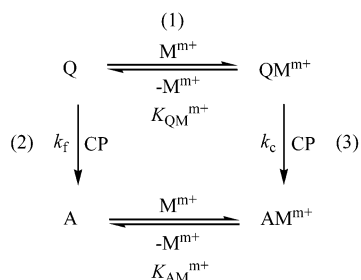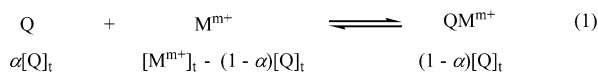
The binding constants K_{QM}^{m+} for complexation of acyclic oligoether quinones with metal cations were estimated by the titration experiments of UV−visible spectroscopic change due to the complexation of the oligoether quinone with the cation.[15,16] The titration profile of a typical absorption change at
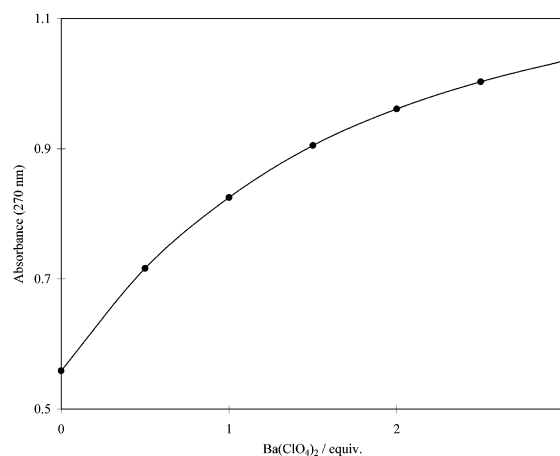

Figure 2. Dependence of the absorption spectrum of **1c** (0.2 mM) at 270 nm on the concentration of $Ba(ClO_4)_2$ (0−0.6 mM) in CH_3CN at 303 K. The A_{obsd} values are plotted against the molar equivalent of added salt.

270 nm by addition of $Ba(ClO_4)_2$ into the MeCN solution containing mono-armed **1c** (0.2 mM) at 303 K is shown in Figure 2, where the absorbance of **1c** at $\lambda_{max} = 270$ nm increases with increasing addition of metal salt. The binding constants K_{QM}^{m+} were determined as the following equation.

$$K_{QM}^{m+} = [QM^{m+}]/[Q][M^{m+}] =$$
$$(A_f - A_{obsd})/(A_{obsd} - A_c)[M^{m+}] \quad (4)$$

where

$$[M^{m+}] = [M^{m+}]_t - [Q]_t(A_f - A_{obsd})/(A_f - A_c) \qquad (5)$$

The A_c values can be obtained from the observed absorbance A_{obsd} values at the point of the large ratio of $[M^{m+}]_t$ to $[Q]_t$, where A_c is the absorbance of the complex of acyclic oligoether quinone with the cation, A_f is that of the free one, and $[Q]_t$ and $[M^{m+}]_t$ are the total concentrations of the quinone and the metal ion, respectively. Under these conditions, $[M^{m+}]$ saturates against $[Q]$; therefore, the A_{obsd} obtained can be regarded as A_c.[5b,17] Using this A_c value, we calculated the K_{QM}^{m+} in eq 4, and the reasonably reliable values of A_c and K_{QM}^{m+} can also be obtained by nonlinear least squares curve-fitting analysis.[15] The obtained 1:1 binding constants for divalent metal cations are compiled in Table 2.

The [2+4] cycloadducts were formed from the DA reaction of free quinone (path 2) or a metal-complexed quinone (path 3) with cyclopentadiene, being characterized by the rate coefficients k_f and k_c, respectively. The observed rate constant k_{obsd} is expressed as eq 6.

(13) (a) Izatt, R. M.; Eatough, D. J.; Christensen, J. J. *Struct. Bonding* **1973**, *16*, 161. (b) Frensdroff, H. K. *J. Am. Chem. Soc.* **1971**, *93*, 600. (c) Cram, D. J.; Cram, J. M. *Acc. Chem. Res.* **1978**, *11*, 8. (d) Kyba, E. P.; Helgeson, R. C.; Madan, K.; Gokel, G. W.; Tarnowski, T. L.; Moor, S. S.; Cram, D. J. *J. Am. Chem. Soc.* **1977**, *99*, 2564.

(14) It is well known that Diels−Alder reactions of quinones with cyclopentadiene give the [4+2] *endo* adducts.[5,28b] The reactions of **1c** with cyclopentadiene in the presence or absence of added metal salts, for example, also afforded *endo* adducts quantitatively. Adduct of **1c**: ^{1}H NMR (270 MHz, CDCl₃) δ = 1.43 (m, 1H, CP), 1.53 (m, 1H, CP), 3.23 (t, *J* = 2.7, 2H, CP), 3.38 (s, 3H, Me), 3.53−3.57 (m, 4H, ether), 3.61−3.72 (m, 6H, ether and Q), 3.83−3.86 (m, 2H, ether), 3.94−3.98 (m, 2H, ether), 5.89 (s, 1H, Q), and 6.07 (m, 2H, CP); IR (KBr) 2925, 1694, 1654, 1601, 1458, 1352, 1238, 1107, 867, 728, and 489 cm⁻¹; FAB-MS *m/z* 335, calcd for C₁₈H₂₂O₆, 334. Anal. Calcd for C₁₈H₂₂O₆: C, 64.66; H, 6.63. Found: C, 64.73; H, 6.81.

(15) (a) Leggett, D. J. *Computational Methods for the Determination of Formation Constants*; Plenum: New York, 1985. (b) Connores, K. A. *Binding Constants*; Wiley: New York, 1987.

(16) Benesi, H.; Hildebrand, J. H. *J. Am. Chem. Soc.* **1949**, *71*, 2703.

(17) Aoyama, Y.; Asakawa, M.; Matsui, Y.; Ogoshi, H. *J. Am. Chem. Soc.* **1991**, *113*, 6233.

Table 1. Rate Accelerations of Diels−Alder Reactions of **1**, **2**, and **3** with Cyclopentadiene in the Presence or Absence of Added Alkali Metal Perchlorates in Acetonitrile at 30 °C[a]

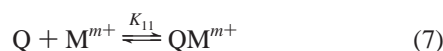| quinone	$10^2 k_f/$ $M^{-1}s^{-1}$ [b]	k_{obsd}/k_f for each additive[c]				
		Li⁺	Na⁺	K⁺	Rb⁺	Cs⁺
1a	2.02	1.13	1.11	1.09	1.09	1.01
1b	2.23	1.07	1.18	1.06	1.16	1.20
1c	2.25	1.20	1.92	1.17	1.16	1.23
2a	4.74	1.22	1.18	1.14	1.08	1.03
2b	4.57	1.80	1.39	1.17	1.15	1.05
2c	4.32	3.68	3.45	1.85	1.74	1.39
3	5.33	1.03	1.00	1.04	1.04	1.02

[a] Kinetic reactions were carried out under pseudo-first-order conditions by using a large excess of cyclopentadiene (17.0 mM) with respect to quinones (0.17 mM). The observed second-order rate constants k_{obsd} were the average of at least two measurements. The error limit of the k_{obsd} is ±2%. [b] The k_f values are taken from the metal-free reaction. [c] The 24 equiv excess of alkali metal perchlorate (4.0 mM) with respect to quinones was used. The counteranion perchlorate was omitted.

$$k_{obsd} = \frac{k_f + k_c K_{QM}^{m+}[M^{m+}]}{1 + K_{QM}^{m+}[M^{m+}]} \qquad (6)$$

As a similar procedure for the estimation of A_c, the rate constants k_c can also be obtained from the k_{obsd} values at the saturated concentration of $[QM^{m+}]$, which is confirmed by the kinetic experiments with varying cation concentration. The produced [4+2] adducts (A) may have little effect on binding constants ($K_{QM}^{m+} \cong K_{AM}^{m+}$), because the observed pseudo-first-order rate constants were not affected during the reactions by their adduct formation even in the various concentrations of the metal ion (an excellent correlation coefficient is always attained, $r >$ 0.999).

For most of the combinations of acyclic oligoether quinones and metal cations, the binding constants K_{QM}^{m+} and the rate constants k_c of DA reactions could be calculated by the above procedures. Therefore, complexation of the acyclic oligoether quinones with the cations proceeds mainly with 1:1 stoichiometry despite the large flexibility of the open-chain oligoethers. However, formations of 1:2 host−guest complexes were confirmed in the largest quinone **2c**.

1:2 Host−Guest Complexation. Although most of the combinations of quinones and cations constructed the 1:1 complexes in good accordance with the above equations, additions of divalent perchlorates such as Ca²⁺, Sr²⁺, and Ba²⁺ into the CH₃CN solution of acyclic ligand **2c** resulted in a significant change in the UV−visible spectrum to afford profiles which were clearly different from 1:1 complexation (Scheme 2). For example, the complexation of **2c** with Ca²⁺ brought about an absorption increase at around 273 nm, and the plot of the increase for the concentration of the added metal salt provided a profile having two saturation points (Figure 3a). Such a spectroscopic change until the first saturation may be interpreted as formation of the 1:1 **2c**·Ca²⁺ complex, and the absorption increase by further addition of Ca²⁺ salt until the second saturation may be attributable to the 1:2 **2c**·(Ca²⁺)₂ complex.

$$Q + M^{m+} \underset{}{\overset{K_{11}}{\rightleftharpoons}} QM^{m+} \qquad (7)$$

$$QM^{m+} + M^{m+} \underset{}{\overset{K_{12}}{\rightleftharpoons}} Q(M^{m+})_2 \qquad (8)$$

Table 2. Rate Accelerations of Diels−Alder Reactions of **1**, **2**, **3**, and **4** with Cyclopentadiene in the Presence of Alkaline Earth Metal Perchlorate in Acetonitrile at 30 °C and Equilibrium and Rate Constants[a]

quinone	cation[b]		$k_c/M^{-1}s^{-1}$ [c]	$\log K_{QM}^{2+}$	k_c/k_f
1a	Mg²⁺		d	d	
	Ca²⁺		d	d	
	Sr²⁺		d	d	
	Ba²⁺		d	d	
1b	Mg²⁺		d	d	
	Ca²⁺		6.94	2.45	311
	Sr²⁺		1.79	2.14	80.3
	Ba²⁺		0.84	2.12	37.7
1c	Mg²⁺		8.69	0.79	386
	Ca²⁺		7.35	3.13	327
	Sr²⁺		1.83	3.39	82.1
	Ba²⁺		0.88	3.70	39.5
2a	Mg²⁺		d	d	
	Ca²⁺		d	d	
	Sr²⁺		d	d	
	Ba²⁺		d	d	
2b	Mg²⁺		d	d	
	Ca²⁺		6.85	3.53	150
	Sr²⁺		1.73	3.03	37.9
	Ba²⁺		0.87	3.57	19.0
2c	Mg²⁺		50.2	2.38	1162
	Ca²⁺	(1:1)	4.13	5.09	95.6
		(1:2)	15.4	1.97	356
	Sr²⁺	(1:1)	1.70	4.49	39.4
		(1:2)	4.65	2.01	108
	Ba²⁺	(1:1)	0.48	5.75	11.1
		(1:2)	3.51	1.33	81.3
3	Mg²⁺		d	d	
	Ca²⁺		d	d	
	Sr²⁺		d	d	
	Ba²⁺		d	d	
4a[e]	Mg²⁺		0.44	2.65	8.4
	Ca²⁺		0.62	4.11	12.0
	Sr²⁺		0.51	4.72	9.8
	Ba²⁺		0.32	4.62	6.2
4b[e]	Mg²⁺		d	d	
	Ca²⁺		0.34	5.28	7.3
	Sr²⁺		0.56	5.33	12.2
	Ba²⁺		0.47	6.33	10.2
4c[e]	Mg²⁺		7.71	2.11	162
	Ca²⁺		0.81	4.93	17.0
	Sr²⁺		0.25	5.02	5.3
	Ba²⁺		0.35	5.64	7.3

[a] Kinetic reactions were carried out under pseudo-first-order conditions by using 10−100 equiv excess of cyclopentadiene (2.0−17.0 mM) with respect to quinones (0.17 mM). [b] Counteranion perchlorate is omitted. [c] The k_c values are obtained from k_{obsd} at the saturation point of $[Q·M^{2+}]$. The observed second-order rate constants k_{obsd} were the average of at least two measurements. The error limit of the k_{obsd} is ±2%. [d] No applicable absorption change and rate acceleration to calculate $\log K_{QM}^{2+}$ and k_c were observed. [e] These values were used from our previous paper (ref 5b).

The much larger K_{11} value which disregards the 1:2 complexation in eq 7 can be calculated by the procedure employed for 1:1 complexation as described above. The K_{12} value in eq 8 can also be determined by using this K_{11} value as follows.[18] The absorbance A_{obsd} at 273 nm of the complex **2c**·(Ca²⁺)₂ can be expressed by eq 9, where A_0 and A_1 are the absorbances of free **2c** and of the 1:1 complex **2c**·Ca²⁺, respectively, and A_2 is the absorbance of the 1:2 complex **2c**·(Ca²⁺)₂ in the presence of a large excess of Ca²⁺. Equation 9 can be rewritten as eq 10. Because the value of the left-hand side in eq 10 is obtained by using the K_{11} value, the K_{12} value can be determined from the slope of a linear plot between the left-hand side in eq 10 and $(A_2 - A_{obsd})[Ca^{2+}]$ (Figure 3b). From this procedure, we

(18) Fukuzumi, S.; Kondo, Y.; Mochizuki, S.; Tanaka, T. *J. Chem. Soc., Perkin Trans. 2* **1989**, 1753.

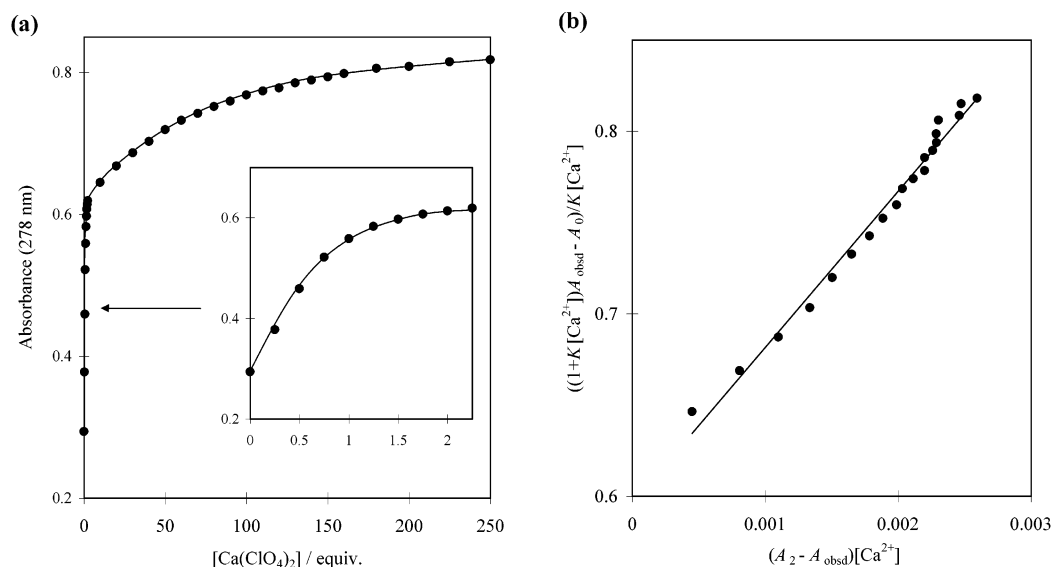**Figure 3.** (a) Dependence of the absorption spectrum of **2c** (0.2 mM) at 278 nm on the concentration of Ca(ClO$_4$)$_2$ (0−50 mM) in CH$_3$CN at 303 K. (b) Plot of $((1 + K[Ca^{2+}])A_{obsd} - A_0)/K[Ca^{2+}]$ versus $(A_2 - A_{obsd})[Ca^{2+}]$. Observed slope = 85.1, intercept = 0.60, and r^2 = 0.986.

could obtain the binding constants of log K_{11} = 5.09 and log K_{12} = 1.93 for the 1:1 and 1:2 complexes **2c·Ca^{2+}** and **2c·(Ca^{2+})$_2$**, respectively. The obtained 1:2 binding constants K_{11} for the other divalent Sr^{2+} and Ba^{2+} are also listed in Table 2.

$$A_{obs} = \frac{A_0 + K_{11}[M^{m+}]A_1 + K_{11}K_{12}[M^{m+}]^2 A_2}{1 + K_{11}[M^{m+}] + K_{11}K_{12}[M^{m+}]^2} \quad (9)$$

$$\frac{(1 + K_{11}[M^{m+}])A_{obs} - A_0}{K_{11}[M^{m+}]} = K_{12}(A_2 - A_{obs})[M^{m+}] + A_1 \quad (10)$$

With respect to the k_{obsd} under the formation of 1:2 complex **2c·(M^{2+})$_2$**, we can express them as being similar to eqs 9 and 10, in which the absorbance A is altered to the rate constant k, because all of the kinetic profiles obtained were fundamentally in agreement with the respective UV−visible titration profiles.

Plausible Complex Structures Based on ^{1}H NMR Spectral Analysis. The complexations of cyclic or acyclic oligoethers with metal cations generally bring about downfield shifts of the ^{1}H NMR signals of the host molecules, whose magnitudes depend mainly on the geometrical location of the cation in the complex produced.[19] As clear examples, we investigated the complex structures of **1c·Ba^{2+}** and **2c·Ba^{2+}** in comparison with the size-fitted quinocrown ether complex **4b·Ba^{2+}** as a reference in the ^{1}H NMR spectroscopy.

The reference **4b·Ba^{2+}** exhibited the larger downfield shifts at the crown ether moiety ($\Delta\delta$ = 0.18−0.27 ppm) than at the vinyl protons of quinone (0.08 ppm) (Scheme 3). This is because the incorporated metal cation can directly interact with the crown ether oxygen atoms, but indirectly exerts the Lewis acidity to the remote part of the quinone.

In contrast, mono-armed **1c·Ba^{2+}** showed comparable larger downfield shifts for both the oligoether ethylene ($\Delta\delta$ = 0.16−0.21 ppm) and the quinone vinyl protons (0.14−0.17 ppm). These NMR chemical shifts indicate formation of the lariat-shaped complex as shown in Scheme 3, in which one of the

quinone carbonyl groups actually participates in the cation binding by judging from the enhanced downfield shifts at the vinyl protons. The magnitudes of the downfield shifts in the order of 3-position ($\Delta\delta$ = 0.17 ppm) > 6-position (0.15) > 5-position (0.14) are in harmony with the efficiency in the cation-induced electron withdrawal through the π-resonate carbonyl group (1-position) and the adjacent alkoxy linkage (2-position).

Interestingly, di-armed **2c** displayed two-step saturation with Ba^{2+}, which corresponds to the formations of 1:1 and 1:2 complexes, as is also observed in the UV/vis titration experiments of the absorption spectrum (Supporting Information). At the first saturation, which was achieved by the addition of ca. 1 equiv of Ba^{2+}, larger downfield shifts were observed for the two oligoether moieties ($\Delta\delta$ = 0.17−0.23 ppm) relative to the quinone protons (0.12 ppm) (Scheme 3). The quinone protons of **2c·Ba^{2+}** exhibited a larger downfield shift by 0.04 ppm than those of **4b·Ba^{2+}**, but a smaller shift by 0.02−0.03 ppm than those of **1c·Ba^{2+}**. These observations and its large binding constant (log K_{QM}^{2+} = 5.75) suggest that **2c** preferentially accommodates Ba^{2+} in the highly flexible pseudo-cyclic cavity constructed by the two oligoether chains probably with a little participation of the carbonyl oxygen to the complexations. At the second saturation which was attained by the addition of ca. 200 equiv of Ba^{2+}, a larger downfield shift from the 1:1 complexation was noticed for the quinone protons ($\Delta\delta$ = 0.15 ppm), although small shifts were observed for the oligoether moiety (−0.05−0.03 ppm). This enhanced downfield shift at quinone strongly indicates formation of 1:2 complex **2c·(Ba^{2+})$_2$**, where two carbonyl oxygens take part in the cation binding (Scheme 3).[20] In fact, this total chemical shift at quinone ($\Delta\delta$ = 0.27 ppm) is well consistent with the expected value ($\Delta\delta$ = 0.29 ppm) for the bis-lariat complex by summation of the relevant values of **1c·Ba^{2+}** (0.15 and 0.14 ppm for 5- and 6-positions, respectively). However, such 1:2 binding behavior

(19) Ikeda, A.; Shinkai, S. *Chem Rev.* **1997**, *97*, 1713.

(20) (a) Echegoyen, L.; Kaifer, A.; Durst, H.; Schultz, R. A.; Dishong, D. M.; Goli, D. M.; Gokel, G. W. *J. Am. Chem. Soc.* **1984**, *106*, 5100. (b) Schultz, R. A.; White, B. D.; Dishong, D. M.; Arnold, D. K.; Gokel, G. W. *J. Am. Chem. Soc.* **1985**, *107*, 6659. (c) Miller, S. R.; Gustowski, D. A.; Gokel, G. W.; Echegoyen, L.; Kaifer, A. E. *Anal. Chem.* **1988**, *60*, 2021.

Scheme 3. Observed Shifts (ppm) of ^{1}H NMR (500 MHz) Signals of **1c**, **2c**, and **4b** by Addition of Ba(ClO$_4$)$_2$ in CDCl$_3$ at 25 °C and Their Possible Complexation Structures Suggested from these Shifts
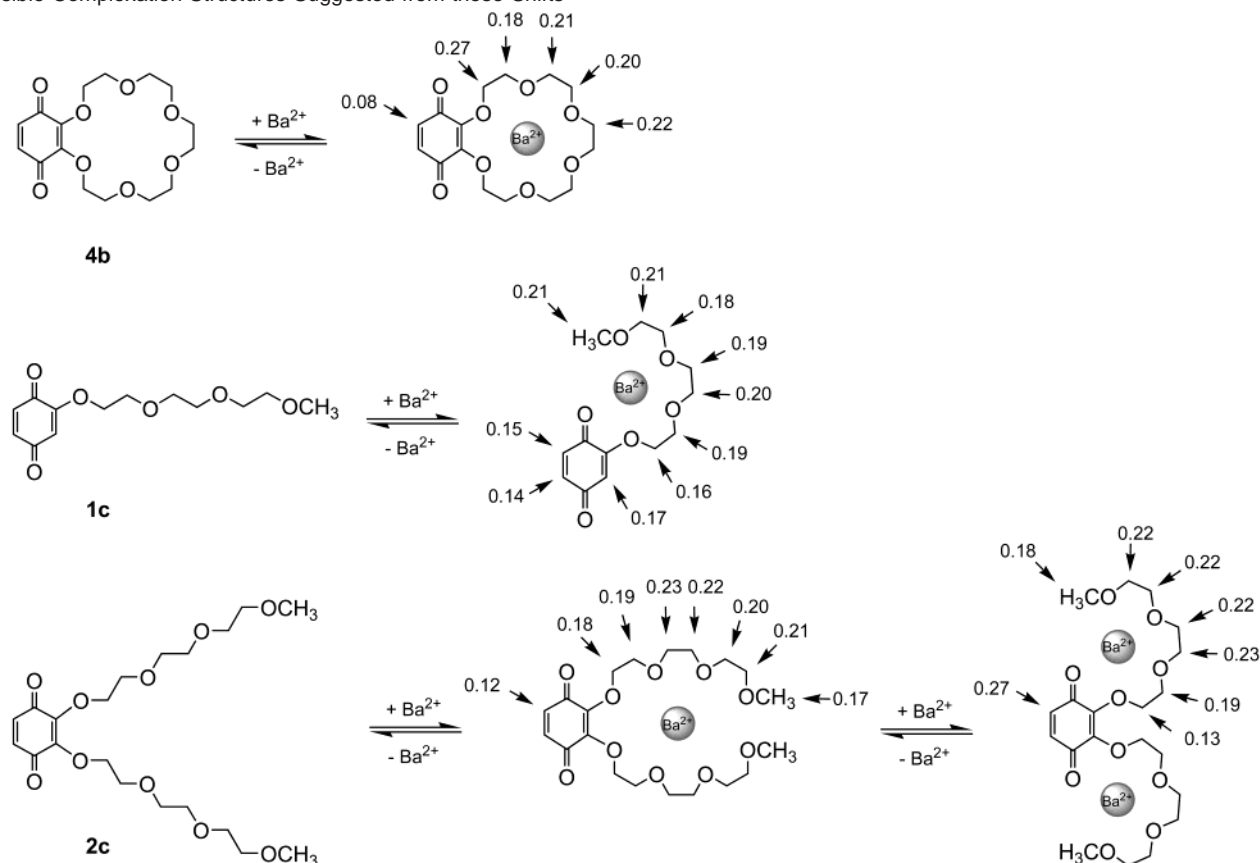
was extremely reduced in **2b** (Supporting Information), in which its respective shorter sidearms cannot strongly bind Ba^{2+} as expected from mono-armed **1b**·Ba^{2+}.

In the following sections, we will discuss the effects of cation binding on DA reactions of acyclic oligoether quinones with cyclopentadiene on the basis of complexation features described above.

Measurements of Reaction Rates. The kinetic experiments were performed in an acetonitrile solution containing a quinone (0.17 mM) and a large excess of cyclopentadiene (2.0–16.0 mM) with or without addition of alkali, alkaline earth metal perchlorates, or scandium triflate at 303 K. The rates of reactions were determined by monitoring the disappearance of absorbances due to quinones **1a**–**c** at $\lambda_{max} = 360$ nm, and **2a**–**c** and **3** at $\lambda_{max} = 391$–399 nm. The rates obeyed pseudo-first-order kinetics up to at least two half-lives, and the second-order rate constants were obtained by dividing the observed first-order rate constants by the corrected concentration of cyclopentadiene on the consumption of a half-amount of quinone. In the absence of metal salts, the second-order rate constants varied in the range of 2.0–2.3 × 10^{-2} M^{-1} s^{-1} for **1a**–**c**, and 4.3–5.3 × 10^{-2} M^{-1} s^{-1} for **2a**–**c** and **3**. The addition of metal salts brought about more or less the rate enhancement depending on the combination of quinones and metal cations. The details will be described for the univalent, divalent, and trivalent metal complexations, respectively.

Univalent Cation Recognition. Initially, we performed a systematic kinetic experiment for DA reactions accelerated by the univalent cation recognition with the fixed concentration of host quinone and guest metal ion because of poor complex-

ation ability. The experiments were carried out in MeCN solution containing an acyclic oligoether quinone (0.17 mM) with a large excess of cyclopentadiene (17 mM) with or without added 24 equiv excess of alkali metal perchlorate (4 mM) at 303 K.

In the absence of metal perchlorate, DA reactions of mono-armed quinones **1a**–**c**, di-armed **2a**–**c**, and reference **3** with cyclopentadiene gave the rate constants $k_f = 2.0$–2.2 × 10^{-2}, 4.3–4.7 × 10^{-2}, and 5.3 × 10^{-2} M^{-1} s^{-1}, respectively. The lower reactivity of **1a**–**c**, about one-half that of **2a**–**c** and **3**, is probably due to the reduced inductive effects by the mono-armed oxygen atom, which would result in the poor drop of the quinone LUMO energy. In the presence of univalent metal salts, the quinones **1c**, **2b**, and **2c** bearing relatively longer oligoether chains undergo more or less the selective rate enhancement of [4+2] cycloaddition reflecting their characteristic complexations (Table 1). The overall kinetic features associated with the cation binding can be more explicitly visualized in the plots of $\ln(k_{obsd}/k_f)$ versus metal ion radius (Figure 4). The most selective acceleration for each quinone was attained for the complexes **1c**·Na$^+$ ($k_{obsd}/k_f = 1.9$), **2b**·Li$^+$ (1.8), and **2c**·Li$^+$ (3.7). Contrary to these long-armed quinones, short-armed quinones **1a**, **1b**, **2a**, and reference **3** showed no appreciable rate dependency on the addition of metal salts because of their weak cation affinities. It was also noted that the conspicuous selective accelerations, which were predicted from the size-fit concept on the previous studies of crown ethers, were not observed for both families of quinones **1** and **2**.[5,21] Larger acceleration seems to be achieved in the combinations of larger oligoether quinones and smaller cations.
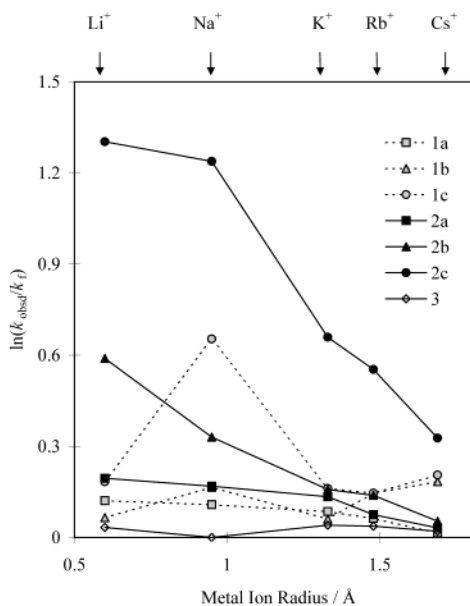
Figure 4. Plot of $\ln(k_{obsd}/k_f)$ versus the alkali metal ion radius (Å), where k_{obsd} and k_f represent the rate constants for the reactions in the presence and absence of added alkali metal perchlorates (4.0 mM), respectively. Metal ion radii (Å): $Li^+ = 0.60$, $Na^+ = 0.95$, $K^+ = 1.33$, $Rb^+ = 1.48$, $Cs^+ = 1.69$.

For $2c \cdot Li^+$ and $2c \cdot Na^+$ complexes, which exhibited larger k_{obsd}/k_f, the binding constants with 1:1 stoichiometry and the rate constants k_c were determined from the titration profiles of the absorption spectra and the concentration-dependent kinetic profiles of DA reactions, respectively. The $2c \cdot Li^+$ complex has a small binding constant of $\log K_{2c \cdot Li^+} = 1.28$ and a larger rate constant of $k_c = 1.03$ M^{-1} s^{-1} ($k_c/k_f = 23.4$) as compared with the size-fitted quinocrown complex $4b \cdot K^+$ ($k_c = 0.17$ M^{-1} s^{-1} ($k_c/k_f = 3.7$)).[5] The pronounced rate enhancement in $2c \cdot Li^+$ may be attributed to the cooperative participation of the quinone carbonyl oxygen to the metal complexation, by which the bound cation may exert effective electron-withdrawing ability on the conjugated C=C bond of quinone (vide infra).[22] Similar curve fitting provided $\log K_{2c \cdot Na^+} = 1.97$ and $k_c = 0.28$ M^{-1} s^{-1} ($k_c/k_f = 6.39$) for the $2c \cdot Na^+$ complex. The more favorable acceleration for $2c \cdot Li^+$ than $2c \cdot Na^+$ may be explained by the more effective electron withdrawal by the smallest Li^+ cation. Thus, the smaller k_c but larger $K_{2c \cdot Na^+}$ of $2c \cdot Na^+$ as compared with that of the $2c \cdot Li^+$ complex implies that the larger Na^+ cation is more favorably accommodated in the pseudo-cyclic cavity of $1c$ than Li^+, but exerts reduced electron withdrawal on account of the weaker Lewis acidity.

These observations indicate that the suitable pseudo-cyclic complexation of a smaller cation with the aid of a quinone carbonyl interaction would result in the more enhanced rate acceleration as deduced from Figure 4. In the next section, the detailed relationships between rate acceleration and cation recognition will be described in view of the k_c, K_{QM}^{m+}, metal cation size, and chain length.
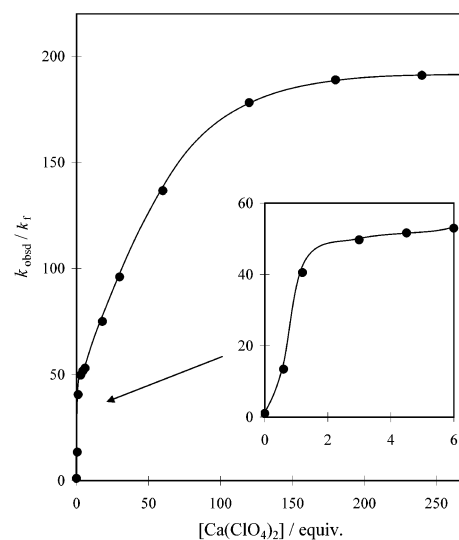
(21) (a) Izatt, R. M.; Bradshaw, J. S.; Nielson, S. A.; Lamb, J. D.; Christensen, J. J. *Chem. Rev.* **1985**, *85*, 271. (b) Bajaj, A. V.; Poonia, N. S. *Coord. Chem. Rev.* **1988**, *87*, 55. (c) Izatt, R. M.; Pawlak, K.; Bradshaw, J. S.; Bruenig, R. L. *Chem. Rev.* **1991**, *91*, 1721.
(22) The carbonyl oxygens of quinones have a large affinitiy for metal cations. Their interactions, where metal cations act as Lewis acid, have been applied to the catalysis of various organic reactions. (a) Fukuzumi, S.; Okamoto, T. *J. Am. Chem. Soc.* **1993**, *115*, 11600. (b) Vaugeois, J.; Wuest, J. D. *J. Am. Chem. Soc.* **1998**, *120*, 13016.

Figure 5. Dependence of k_{obsd} on the concentration of $Ca(ClO_4)_2$ (0−45 mM) for the Diels−Alder reaction of $2c$ (0.17 mM) with cyclopentadiene (2.0 mM) in CH_3CN at 303 K.

Divalent Cation Recognition. Effects of Binding Constants, Geometry, and Stoichiometry. The complexation of quinones $1b$, $1c$, $2b$, and $2c$ with alkaline earth metal ions brought about much larger rate accelerations ($k_c/k_f = 11-1162$) as compared with the univalent alkali metal complexes or size-fitted quinocrown ether complexes such as $4a \cdot Ca^{2+}$ ($k_c/k_f = 12.0$) and $4b \cdot Ba^{2+}$ (10.2) (Table 2).[5] However, the short-armed quinones $1a$ and $2a$ as well as reference 3 showed no applicable acceleration due to their weak cation affinities ($k_{obs}/k_f = 1.0-1.4$ even in the presence of 10 equiv of metal cations). The binding constants K_{QM}^{2+} were determined by titration experiments of the absorption spectra, and the saturated rate constants k_c of the DA reactions of the complexes with cyclopentadiene were also estimated by the saturation point on kinetic profiles. With respect to the complexation stoichiometry, these oligoether quinones $1b$, $1c$, and $2b$ interacted with divalent cations to form the 1:1 noncovalent complexes, whereas $2c$ formed the 1:1 and then 1:2 complexes with Ca^{2+}, Sr^{2+}, Ba^{2+} as indicated by the ^1H NMR and UV/vis spectroscopy. Such 1:2 complexations were also observed in the kinetic profiles of $2c$ on varying the concentration of divalent cations, as represented for Ca^{2+} (Figure 5). The rate constants for the 1:1 and 1:2 complexes ($k_{c(1:1)}$ and $k_{c(1:2)}$) can be determined from the respective saturation points in the plots of k_{obsd} versus metal salt concentrations (Table 2).

$\log K_{QM}^{2+}$ **versus Metal Ion Radius.** A plot of complexation stabilities ($\log K_{QM}^{2+}$) against the metal ion radius (Å) revealed some tendencies in the rate enhancements (Figure 6). In all of the divalent metal complexes, the largest K_{QM}^{2+} with 1:1 bindings was achieved by $2c$. The increased binding constants from $1b$ to $1c$ and from $2b$ to $2c$ are also observed for all of the metal complexes. The more the host moiety enlarges with increasing oxyethylene units, the more the cation capturing ability of the acyclic host moiety becomes advantageous. However, despite the small number of donor oxygens, the mono-armed $1c$, which may construct lariat-shaped complexes by using five donor oxygens, displays a similar binding profile to di-armed $2b$ having six effective oxygens and further can form a complex with smaller Mg^{2+}. In addition, although $1b$ and $2a$ may have the same number of effective oxygens for complexations, only mono-armed $1b$ can form complexes with Ca^{2+},
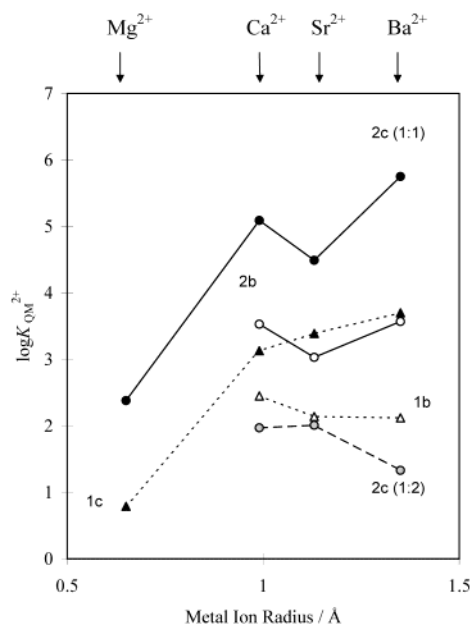
Figure 6. Plot of log K_{QM}^{2+} versus ion radius (Å) for the divalent metal complexes of **1b**, **1c**, **2b**, and **2c** (including 1:1 and 1:2). Metal ion radii (Å): $Mg^{2+} = 0.65$, $Ca^{2+} = 0.99$, $Sr^{2+} = 1.13$, $Ba^{2+} = 1.35$.

Figure 7. Plot of $\ln(k_c/k_f)$ versus ion radius (Å) for the divalent metal complexes of **1b**, **1c**, **2b**, and **2c** (including 1:1 and 1:2).

Sr^{2+}, and Ba^{2+} with small K_{QM}^{2+}. These observations indicate that the Lewis basicity of quinone carbonyl oxygen is larger than that of oligoether oxygens for the complexations. Such a strong basicity of carbonyl oxygens may also allow for the formation of 1:2 complexes in **2c**.

In these acyclic oligoether quinones, the cation selectivity is quite low as compared with that of quinocrown ethers; that is, the affinity between host and guest is scarcely affected by variation of the cation size. These acyclic oligoether quinones having large flexibilities can meet the structural demand from guest cations for the complexations; in contrast, the quinocrowns **4** cannot accept it due to the restricted flexibility of the cyclic structures.

$\ln(k_c/k_f)$ versus Metal Ion Radius. In the plots of $\ln(k_c/k_f)$ versus metal ion radius in Figure 7, it is found that 1:2 **2c·**$(M^{2+})_2$ complexes for Ca^{2+}, Sr^{2+}, or Ba^{2+} ions are the most effective for the acceleration of DA reactions (Table 2). On the contrary, acceleration of the corresponding 1:1 **2c·**M^{2+} complexes is less effective for these cations. In comparison of the rate enhancements of 1:1 complexes, mono-sidearms **1b·**M^{2+} and **1c·**M^{2+} exhibit the largest acceleration for Ca^{2+}, Sr^{2+}, and Ba^{2+}. **1b** and **1c** have different affinities for these cations, but provide quite similar kinetic profiles, in which their accelerations are also larger than those of di-sidearms **2b·**M^{2+} and **2c·**M^{2+}, and quinocrown **4·**M^{2+} complexes. There are probably little differences among the basic complexation structures of **1b** and **1c** with Ca^{2+}, Sr^{2+}, and Ba^{2+}; thus, they may adopt the lariat-shaped complexations as shown in Scheme 3. The larger contribution of quinone carbonyl oxygen to the complexation may lead to more effective electron withdrawing from the quinone moiety, resulting in larger accelerations. The smaller k_c of **2b** and **2c** as compared with that of **1b** and **1c**, and further the more declined k_c of **2c** than that of **2b**, may result from interference of the interaction between quinone carbonyl oxygen and chain-bound cation due to the effective encapsulation of the cation by the two oligoether sidearms. As shown in the
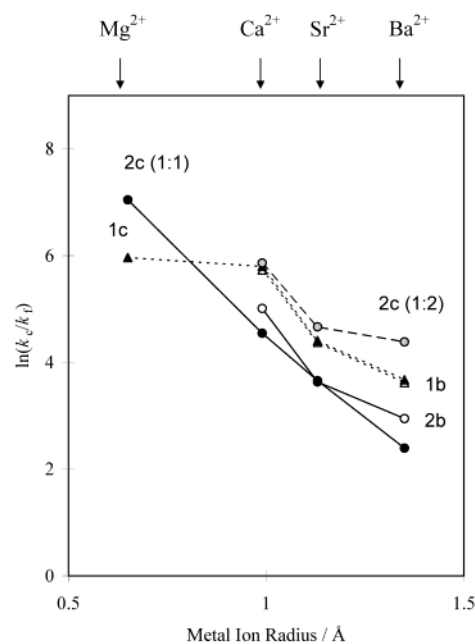
quinocrown ethers reported previously, the strong accommodation of the guest cation by the crown ether ring is ineffective for the rate enhancement, although selective acceleration was achieved as a result of their selective cation binding (Table 2).[5]

It should be noted that long-armed **1c** and **2c** only can bind Mg^{2+}, bringing about larger rate accelerations. The charge condensed Mg^{2+} cation is a potential strong Lewis acid, and thus the **1c·**Mg^{2+} complex that is stabilized by the contribution of quinone carbonyl oxygen, as described above, can produce larger rate acceleration. In all of the divalent complexes, **2c·**Mg^{2+} that exhibits only 1:1 stoichiometry displays the largest acceleration. The additional sidearm of **2c** may be able to assist more appropriate interactions between Mg^{2+} and carbonyl oxygen as compared with **1c**, resulting in the largest k_c. This long-arm effect was also observed in the quinocrown **4c·**Mg^{2+} complex, which displayed the largest acceleration in divalent quinocrown complexes **4·**M^{2+}.

As another observation, the rate accelerations by complexations of acyclic oligoether quinones with divalent cations show a global tendency in which the smaller cation seems to give a larger acceleration for all of the oligoether quinones (Figure 7), similar to the case of univalent cations (Figure 4). In all cases, including 1:2 **2c·**$(M^{2+})_2$ complexes, this tendency can be observed. This trend may be ascribed to the different Lewis acidity of the cations.[23] There are many reports for the studies of electrochemical behavior of functionalized quinones bearing host moieties such as crown and podand in the presence of metal cations.[24] Their complexations were accelerated by the ionic interaction of reduced quinone with metal cations upon electrochemical reduction. In comparisons of the complex stabilities of the neutral quinonoid hosts and their reduced forms with alkali metal cations, the smaller metal cation provided larger complexation stability in all cases. This observed trend in the electrochemical behavior of functionalized quinones is attributable to the different charge densities of metal cations and is

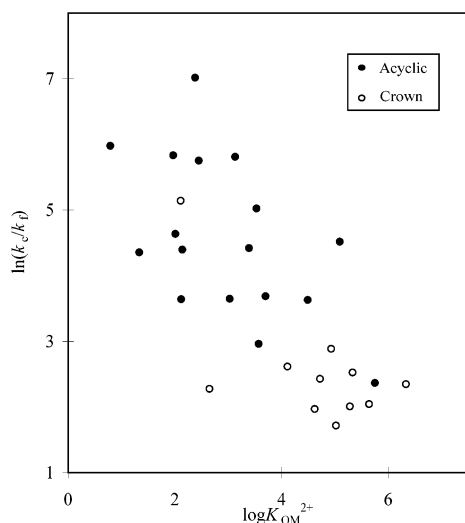(23) Fukuzumi, S.; Okubo, K. *Chem.-Eur. J.* **2000**, *6*, 4532.

Figure 8. Plot of $\ln(k_c/k_f)$ versus $\log K_{QM}^{2+}$ for the divalent metal complexes of **1b**, **1c**, **2b**, **2c** (including 1:1 and 1:2), and **4a−d**.

Table 3. Rate Accelerations of Diels−Alder Reactions of **1**, **2**, **3**, and **4** with Cyclopentadiene in the Presence of Sc(OTf)$_3$ in Acetonitrile at 30 °C and Equilibrium and Rate Constants[a]

quinone	$k_c/M^{-1}s^{-1}$ [b]	$\log K_{QM}^{2+}$ [c]	k_c/k_f
1a	*d*		*d*
1b	677	3.2	14 800
1c	4090	5.0	182 000
2a	*d*		*d*
2b	38.2	4.8	1710
2c	8280	4.9	192 000
3	(1.46)[e]		(27.3)[e]
4a[f]	96.2	2.4	2021
4b[f]	46.5	2.7	977
4c[f]	4.92	4.8	103

[a] Kinetic reactions were carried out under pseudo-first-order conditions by using 10−100 equiv excess of cyclopentadiene (0.5−5.0 mM) with respect to quinones (0.05 mM). [b] The k_c values are obtained from k_{obsd} at the saturation point of [Q·Sc^{3+}]. The observed second-order rate constants k_{obsd} were the average of at least two measurements. The error limit of the k_{obsd} is ±2%. [c] Approximate binding constants were calculated from kinetic profiles. [d] No applicable rate acceleration to calculate k_c was observed. [e] The value in parentheses is k_{obsd} for the cycloaddition of **3** (0.17 mM) in the presence of 24 equiv excess of Sc(OTf)$_3$ (4.0 mM). [f] These values were used in our previous paper (ref 5b).

entirely similar to our study on rate accelerations. Hence, the combination of a flexible oligoether quinone, which can assist the metal−carbonyl interaction, and a smaller metal cation with larger electron density, brings about effective electron withdrawal associated with the larger acceleration.

$\ln(k_c/k_f)$ versus $\log K_{QM}^{2+}$. The overall kinetic features of accelerations of DA reactions by divalent cation recognitions can be more clearly understood in Figure 8, where $\ln(k_c/k_f)$ values for all of the complexes of **1**, **2**, and **4** are plotted against $\log K_{QM}^{2+}$. This plot clarifies a global trend of contribution of the complex stability to the rate acceleration. As a characteristic observation, it can be found that the smaller binding constant of host−guest complexation that can increase interaction between carbonyl oxygens and the incorporated cation is necessary to cause larger rate enhancement. Therefore, the acyclic oligoether quinones, which have larger flexibility as well as smaller affinities for metal cations, are more advantageous for rate accelerations than are quinocrown ethers **4**. The restricted cyclic chain in quinocrowns **4** is favorable for selective cation binding, which is associated with the selective rate acceleration, but is unfavorable to cause dramatic acceleration. As an exception, **4c·Mg^{2+}** bearing larger flexibility with a smaller binding constant displays the anomalous larger acceleration like oligoether quinones. By following this consideration, the largest acceleration is expected to be achieved in shorter-armed **1a**, **2a**, and reference **3**; however, no acceleration was observed due to their extremely poor binding affinity for all of the cations. This global tendency for larger acceleration from Figure 8 indicates the importance of complex structures and their stabilities for the rate accelerations.

Trivalent Sc^{3+} Recognition. Abnormal Accelerations by Sc^{3+} Recognition. Recently, rare-earth metal triflates are well known as effective catalysts for a variety of organic reactions, where these metal salts mainly act as a strong Lewis acid.[25] In particular, among them, Sc^{3+} has displayed excellent catalytic activity due to its smaller ion size (ion radius = 0.81 Å) and hard metal character. For example, oxidative ring-closed reactions of porphyrin oligomers with 2,3-dichloro-5,6-dicyano-*p*-benzoquinone (DDQ) proceeded only in the presence of Sc(OTf)$_3$, where Sc^{3+} interacts with the quinone carbonyl oxygens to stabilize the intermediate quinone anion radical.[26]

The DA reactions of acyclic oligoether quinones **1b**, **1c**, **2b**, and **2c** with cyclopentadiene were dramatically accelerated by addition of trivalent Sc^{3+} (k_c/k_f = 1710−192 000), although the k_c values for the short-armed **1a**, **2a**, and **3** could not be calculated because of the poor host−guest interaction (Table 3). The highest k_c/k_f value of 192 000 for **2c** corresponds to the enormous reduction of the activation energy by 30.7 kJ mol^{-1}, which amounts to 60% of the uncatalyzed reaction ($\Delta G^{\ddagger}$ = 51.6 kJ mol^{-1}). This Sc^{3+} catalyzed acceleration, which is much larger than that for quinocrown ethers **4** (k_c/k_f = 103−2020), strongly supporting the participation of quinone carbonyl oxygen in the lariat complexation. Unfortunately, their reliable binding constants could not be determined by the titration experiments in the absorption spectra because of the gradual degradation of host quinones by added Sc(OTf)$_3$. Hence, approximate binding constants were calculated from their concentration-dependent kinetic profiles. The selected profiles of **1c** and **2c** are shown in Figure 9, where k_{obsd}/k_f values are almost superimposed with the saturation at approximately 3 equiv of added Sc(OTf)$_3$. In contrast to the case of divalent cations, there is no indication of the formation of 1:2 complex as indicated by the plateau values even on further addition of Sc^{3+}.

Absence of 1:2 complex for **2c** can be explained by considering that the 1:1 complexation substantially reduces the electron density of opposite quinone carbonyl oxygen, and a possible 1:2 complex, even if formed, must endure an enormous

(24) (a) Sugihara, K.; Kamiya, H.; Yamaguchi, M.; Kaneda, T.; Misumi, S. *Tetrahedron Lett.* **1981**, *22*, 1619. (b) Bock, H.; Hierholzer, B.; Vögtle, F.; Hollmann, G. *Angew. Chem., Int. Ed. Engl.* **1984**, *23*, 57. (c) Wolf, R. E.; Cooper. S. R. *J. Am. Chem. Soc.* **1984**, *106*, 4646. (d) Maruyama, K.; Sohmiya, H.; Tsukube, H. *Tetrahedron Lett.* **1985**, *26*, 3583. (e) Gustowski, D. A.; Degado, M.; Gatto, V. J.; Echegoyen, L.; Gokel, G. W. *J. Am. Chem. Soc.* **1986**, *108*, 7553. (f) Maruyama, K.; Sohmiya, H.; Tsukube, H. *J. Chem. Soc., Perkin Trans. 1* **1986**, 2069. (g) Deborah, M. D.; Gustowski, D. A.; Yoo, H. K.; Gatto, V. J.; Gokel, G. W.; Echegoyen, L. *J. Am. Chem. Soc.* **1988**, *110*, 119. (h) Togo, H.; Hashimoto, K.; Morihashi, K.; Kikuchi, O. *Bull. Chem. Soc. Jpn.* **1988**, *61*, 3026. (i) Echegoyen, L. E.; Yoo, H. K.; Gotto, V. J.; Gokel, G. W.; Echegoyen, L. *J. Am. Chem. Soc.* **1989**, *111*, 2440.

(25) Kobayashi, S.; Sugiura, M.; Kitagawa, H.; Lam, W. W.-L. *Chem Rev.* **2002**, *102*, 2227.

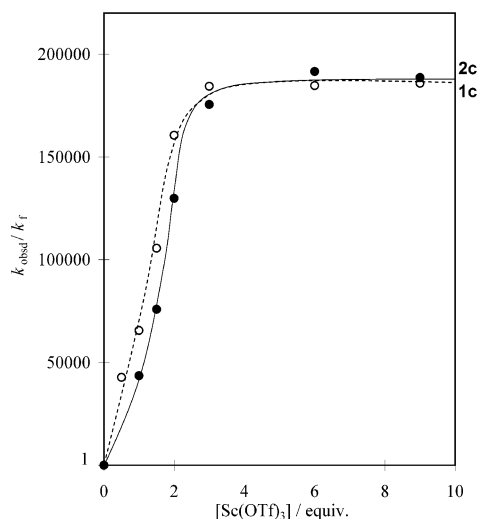(26) Tsuda, A.; Osuka, A. *Science* **2001**, *293*, 79.

Figure 9. Dependence of k_{obsd} on the concentration of Sc(OTf)$_3$ for the Diels−Alder reaction of **1c** and **2c** (0.05 mM) with cyclopentadiene (0.5 mM) in MeCN at 303 K. The k_{obsd} values are plotted against the molar equivalent of added salts.

electrostatic repulsion between the small charge-condensed Sc^{3+} ions. These considerations may be also applied to the lack of the 1:2 complexation between **2c** and the smallest divalent Mg^{2+} (0.65 Å).

The observed differences in acceleration in Sc^{3+} complexes, therefore, can be explained on the basis of the interaction between Sc^{3+} and quinone carbonyl oxygen. The extremely larger rate enhancement (k_c/k_f = 182 000) with larger K_Q·Sc^{3+} in **1c**·Sc^{3+} as compared with that in **1b**·Sc^{3+} (k_c/k_f = 14 800) may be ascribed to the fact that the elongation of one oxyethylene unit in **1c** provides increasing affinity and favorable configurations for the interaction of Sc^{3+} and the carbonyl oxygen in the lariat complexation. The dramatic rate enhancements of **2c**·Sc^{3+} (k_c/k_f = 192 000), thus, can be taken as proving the direct binding of Sc^{3+} on the quinone carbonyl oxygen atom with the aid of two oligoether chains. The drastic decrease of acceleration in shorter two-armed **2b**, which displays smaller 1710-fold acceleration with relatively large K_Q·Sc^{3+}, may result from the difficult Sc^{3+}−carbonyl interaction in **2b**·Sc^{3+} due to the strong encapsulation of Sc^{3+} into the pseudo-cyclic cavity constituted of two oligoether sidearms.

Conclusions

The results presented here for the rate acceleration of the Diels−Alder reaction of metal-complexed oligoether quinones with cyclopentadiene have demonstrated a development of self-activated supramolecules. The noncovalent complexes of oligoether quinones **1** and **2** with metal cations exhibited larger reaction rate accelerations with poor selectivity as compared with those of quinocrown ethers **4**. The large electron withdrawal from the quinone moiety, which is directly associated with the larger rate accelerations, is brought about by the interaction between the quinone carbonyl oxygen and the chain-bound cation. Because strong encapsulation of the metal cation by the host oligoether moiety prevents the interaction of the cation and the quinone carbonyl groups, the larger rate enhancement is achieved in the complexes with weak host−guest interaction. The two-armed **2c**, which has flexible long chains, allowed for the construction of 1:1 and subsequent 1:2 supramolecules with

Ca^{2+}, Sr^{2+}, and Ba^{2+}. Application of these 1:2 complexes to the DA reactions achieved the largest accelerations for all of the metal cations. As another tendency, the complexations of acyclic oligoether quinones with a smaller cation brought about larger rate enhancement, being ascribed to the different charge densities of the metal cations. In comparison of the uni-, di-, and trivalent metal complexes, the valence of the cations is found to be the most effective factor to cause larger rate enhancement. The self-activated supramolecules are expected to have potential utility for catalytic reactions, regio-selective reactions, asymmetric reactions, photonic reactions, and biochemical reactions. These applied studies will be our next fascinating project.

Experimental Section

General. All reagents and solvents were of the commercial reagent grade and were used without further purification except where noted. Dry CH$_2$Cl$_2$ and CHCl$_3$ were obtained by heating under reflux and distillation over CaH$_2$. Solvents used for spectroscopic measurements were all spectroscopic grade. Preparative separations were performed by silica gel gravity-flow column chromatography (Wakogel C-400). Melting points were measured with a Yanagimoto melting-point apparatus. ^{1}H NMR spectra were recorded on a JEOL EX-270 spectrometer and Alpha-500 spectrometer in CDCl$_3$, and chemical shifts were represented as δ values in ppm relative to the internal standard of trimethylsilane (TMS). IR spectra were recorded on a JASCO FT/IR-410 spectrometer. FAB mass spectra were recorded on a JEOL HX-110 spectrometer with the positive-FAB ionization method (accelerating voltage, 10 kV; primary ion sources, Xe) and 3-nitrobenzyl alcohol matrix. Elemental analyses were performed on a Yanaco CHN corder MT-5. UV−visible spectra were recorded on a JASCO V-550 spectrometer equipped with a PELTIER EHC-447 thermostated cell-holder.

Materials. All of the metal perchlorates and triflate were of commercial origin and were used without further purification. Spectrally pure acetonitrile (Nakarai Chemical Co., Ltd.) was used in sample solutions. The compounds **1a−c** and **2b,c** were synthesized by modification of the literature methods.[5,27,28] Cyclopentadiene was purified by distillation just before use. Standard solutions (0.05−1 M) of cyclopentadiene, which was preserved in a freezer, quinones, and metal salts were prepared and subsequently used for kinetic experiments.

Kinetic Measurements. The general kinetic experiments of DA reactions were performed under pseudo-first-order conditions in acetonitrile solution containing a large excess of cyclopentadiene with respect to quinone at 30 °C as described elsewhere.[5b]

2-(2′-Methoxyethoxy)-quinone (1a). Sodium hydroxide (2.4 g, 60 mmol) was added to a stirred solution of 2-benzyloxy-phenol **5** (3.0 g, 15 mmol) and monoethyleneglycol monomethyl ether tosylate **6a** (3.5 g, 15 mmol) in dry dioxane (150 mL), and then the solution was heated at 80 °C for 24 h. The precipitate was filtered off, and the filtrate was evaporated under the reduced pressure to give a viscous residue. The residue was extracted with benzene to give 2-(2′-methoxyethoxy)-1-benzyloxybenzene, **7a** (3.4 g, 88%). Subsequently, a mixture of **7a** and Pd carbon (1 g) in dioxane (10 mL) was stirred under an atmosphere of hydrogen for 3 days. The catalyst was filtered off, and the solvent was evaporated under the reduced pressure to give 2-(2′-methoxyethoxy)phenol, **8a** (2.0 g, 91%), as an oil. Fremy's salt (3.8 g, 14 mmol) was added to a stirred suspension of **8a** (0.55 g, 3 mmol) in 5% aqueous sodium acetate (280 mL) containing a small amount of benzene (30 mL). After the mixture had been stirred at room temperature for 30 min, it was extracted with benzene (3 × 70 mL). The combined organic layers were dried (MgSO$_4$) and concentrated under reduced pressure.

(27) Tsuda, A.; Moriwaki, H.; Oshima, T. *J. Chem. Soc., Perkin Trans. 2* **1999**, 1235.
(28) (a) Dietl, F.; Gierer, G.; Merz, A. *Synthesis* **1985**, 626. (b) Hayakawa, K.; Kido, K.; Kanematu, K. *J. Chem. Soc., Perkin Trans. 1* **1988**, 511.

The residue was chromatographed on a silica gel with benzene−chloroform (3:1), and recrystallized from chloroform−hexane to give **1a** as yellow needles (303 mg, 55%). **1a**: ^{1}H NMR (270 MHz, CDCl$_3$) δ 3.43 (s, 3H, Me), 3.77−3.81 (m, 2H, oxymethylene), 4.05−4.09 (m, 2H, oxymethylene), 5.96 (s, 1H, quinone), 6.69 (s, 1H, quinone), and 6.70 (s, 1H, quinone); IR (KBr) 2942, 2903, 1693, 1658, 1618, 1591, 1478, 1460, 1350, 1315, 1238, 1198, 1128, 1103, 1027, and 876 cm^{-1}; FAB-MS m/z 183 (M + 1), calcd for C$_9$H$_{10}$O$_4$, 182. Anal. Calcd for C$_9$H$_{10}$O$_4$: C, 59.55; H, 5.41. Found: C, 59.34; H, 5.53. mp 65−66 °C; $\lambda_{max}(\epsilon)$ = 358 (1910) nm.

2-(2′-(2″-Methoxyethoxy)ethoxy)-quinone (1b). Sodium hydroxide (2.4 g, 60 mmol) was added to a stirred solution of 2-benzyloxyphenol **5** (3.0 g, 15 mmol) and diethyleneglycol monomethyl ether tosylate **6b** (4.1 g, 15 mmol) in dry dioxane (150 mL), and then the solution was heated at 80 °C for 24 h. The precipitate was filtered off, and the filtrate was evaporated under the reduced pressure to give a viscous residue. The residue was extracted with benzene to give 2-(2′-(2″-methoxyethoxy)ethoxy)-1-benzyloxybenzene, **7b** (4.4 g, 92%). Subsequently, a mixture of **7b** and Pd carbon (1 g) in dioxane (10 mL) was stirred under an atmosphere of hydrogen for 3 days. The catalyst was filtered off, and the solvent was evaporated under the reduced pressure to give 2-(2′-(2″-methoxyethoxy)ethoxy)phenol, **8b** (2.69 g, 88%), as an oil. Fremy's salt (3.8 g, 14 mmol) was added to a stirred suspension of **8b** (0.68 g, 3 mmol) in 5% aqueous sodium acetate (280 mL) containing a small amount of benzene (30 mL). After the mixture had been stirred at room temperature for 30 min, it was extracted with benzene (3 × 70 mL). The combined organic layers were dried (MgSO$_4$) and concentrated under reduced pressure. The residue was chromatographed on a silica gel with benzene−chloroform (1:1). After removal of solvent, **1b** was obtained as a yellow oil (0.39 g, 59%). **1b**: ^{1}H NMR (270 MHz, CDCl$_3$) δ 3.38 (s, 3H, Me), 3.54−3.57 (m, 2H, oxymethylene), 3.69−3.73 (m, 2H, oxymethylene), 3.89−3.92 (m, 2H, oxymethylene), 4.08−4.11 (m, 2H, oxymethylene), 5.96 (s, 1H, quinone), 6.69 (s, 1H, quinone), and 6.70 (s, 1H, quinone); IR (KBr) 2883, 1684, 1654, 1591, 1232, 1100, and 871 cm^{-1}; FAB-MS m/z 227 (M + 1), calcd for C$_{11}$H$_{14}$O$_5$, 226. Anal. Calcd for C$_{11}$H$_{14}$O$_5$: C, 58.40; H, 6.24. Found: C, 58.52; H, 6.43. $\lambda_{max}(\epsilon)$ = 358 (1890) nm.

2-(2′-(2″-(2‴-Methoxyethoxy)ethoxy)ethoxy)-quinone (1c). Sodium hydroxide (2.4 g, 60 mmol) was added to a stirred solution of 2-benzyloxy-phenol, **5** (3.0 g, 15 mmol), and triethyleneglycol monomethyl ether tosylate, **6c** (4.8 g, 15 mmol), in dry dioxane (150 mL), and then the solution was heated at 80 °C for 24 h. The precipitate was filtered off, and the filtrate was evaporated under the reduced pressure to give a viscous residue. The residue was extracted with benzene to give 2-(2′-(2″-(2‴-methoxyethoxy)ethoxy)ethoxy)-1-benzyloxybenzene, **7c** (4.9 g, 94%). Subsequently, a mixture of **6c** and Pd carbon (1 g) in dioxane (10 mL) was stirred under an atmosphere of hydrogen for 3 days. The catalyst was filtered off, and the solvent was evaporated under the reduced pressure to give 2-(2′-(2″-(2‴-methoxyethoxy)ethoxy)ethoxy)phenol, **8c** (3.27 g, 89%), as an oil. Fremy's salt (3.8 g, 14 mmol) was added to a stirred suspension of **8c** (0.81 g, 3 mmol) in 5% aqueous sodium acetate (280 mL) containing a small amount of benzene (30 mL). After the mixture had been stirred at room temperature for 30 min, it was extracted with benzene (3 × 70 mL). The combined organic layers were dried (MgSO$_4$) and concentrated under reduced pressure. The residue was chromatographed on a silica gel with benzene−chloroform (1:3). After removal of solvent, **1c** was obtained as a yellow oil (0.42 g, 52%). **1c**: ^{1}H NMR (270 MHz, CDCl$_3$) δ 3.38 (s, 3H, Me), 3.53−3.57 (m, 2H, oxymethylene), 3.62−3.68 (m, 4H, oxymethylene), 3.70−3.74 (m, 2H, oxymethylene), 3.88−3.92 (m, 2H, oxymethylene), 4.07−4.10 (m, 2H, oxymethylene), 5.96 (s, 1H, quinone), 6.69 (s, 1H, quinone), and 6.70 (s, 1H, quinone); IR (KBr) 2881, 1683, 1654, 1591, 1350, 1308, 1232, 1193, 1099, 942, and 871 cm^{-1}; FAB-MS m/z 271 (M + 1), calcd for C$_{13}$H$_{18}$O$_6$, 270. Anal. Calcd for C$_{13}$H$_{18}$O$_6$: C, 57.77; H, 6.71. Found: C, 57.49; H, 6.65. $\lambda_{max}(\epsilon)$ = 359 (1820) nm.

2,3-Bis(2′-methoxyethoxy)-quinone (2a). Sodium hydroxide (8.0 g, 200 mmol) was added to a stirred solution of 3-benzyloxypyrocatechol **9** (5.0 g, 23 mmol) and monoethyleneglycol monomethyl ether tosylate **6a** (10.6 g, 46 mmol) in dry dioxane (200 mL), and then the solution was heated at 80 °C for 24 h. The precipitate was filtered off, and the filtrate was evaporated under the reduced pressure to give a viscous residue. The residue was extracted with benzene to give 2,3-bis(2′-methoxyethoxy)-1-benzyloxybenzene, **10a** (7.0 g, 91%). Subsequently, a mixture of **10a** and Pd carbon (1 g) in dioxane (10 mL) was stirred under an atmosphere of hydrogen for 3 days. The catalyst was filtered off, and the solvent was evaporated under the reduced pressure to give 2,3-bis(2′-methoxyethoxy)phenol **11a** (4.8 g, 95%) as an oil. Fremy's salt (3.8 g, 14 mmol) was added to a stirred suspension of **11a** (0.77 g, 3 mmol) in 5% aqueous sodium acetate (280 mL) containing a small amount of benzene (30 mL). After the mixture had been stirred at room temperature for 30 min, it was extracted with benzene (3 × 70 mL). The combined organic layers were dried (MgSO$_4$) and concentrated under reduced pressure. The residue was chromatographed on a silica gel with chloroform−THF (49:1). After removal of solvent, **2a** was obtained as a red oil (0.25 g, 32%). **2a**: ^{1}H NMR (270 MHz, CDCl$_3$) δ 3.39 (s, 6H, Me), 3.66−3.69 (m, 4H, oxymethylene), 4.39−4.43 (m, 4H, oxymethylene), and 6.60 (s, 2H, quinone); IR (KBr) 2928, 1657, 1590, 1127, 1075, and 841 cm^{-1}; FAB-MS m/z 257 (M + 1), calcd for C$_{12}$H$_{16}$O$_6$, 256. Anal. Calcd for C$_{12}$H$_{16}$O$_6$: C, 57.34; H, 6.29. Found: C, 57.23; H, 6.12. UV/vis (CHCl$_3$): $\lambda_{max}(\epsilon)$ = 271 (2790) and 399 (1030) nm.

2,3-Bis(2′-(2″-methoxyethoxy)ethoxy)-quinone (2b). Sodium hydroxide (8.0 g, 200 mmol) was added to a stirred solution of 3-benzyloxypyrocatechol, **9** (5.0 g, 23 mmol), and diethyleneglycol monomethyl ether tosylate, **6b** (12.6 g, 46 mmol), in dry dioxane (200 mL), and then the solution was heated at 80 °C for 24 h. The precipitate was filtered off, and the filtrate was evaporated under the reduced pressure to give a viscous residue. The residue was extracted with benzene to give 2,3-bis(2′-(2″-methoxyethoxy)ethoxy)-1-benzyloxybenzene, **10b** (8.6 g, 89%). Subsequently, a mixture of **10b** and Pd carbon (1 g) in dioxane (10 mL) was stirred under an atmosphere of hydrogen for 3 days. The catalyst was filtered off, and the solvent was evaporated under the reduced pressure to give 2,3-bis(2′-(2″-methoxyethoxy)ethoxy)phenol, **11b** (6.3 g, 93%), as an oil. Fremy's salt (3.8 g, 14 mmol) was added to a stirred suspension of **11b** (1.0 g, 3 mmol) in 5% aqueous sodium acetate (280 mL) containing a small amount of benzene (30 mL). After the mixture had been stirred at room temperature for 30 min, it was extracted with benzene (3 × 70 mL). The combined organic layers were dried (MgSO$_4$) and concentrated under reduced pressure. The residue was chromatographed on a silica gel with chloroform−THF (29:1). After removal of solvent, **2b** was obtained as a red oil (0.38 g, 38%). **2b**: ^{1}H NMR (270 MHz, CDCl$_3$) δ 3.36 (s, 6H, Me), 3.50−3.53 (m, 4H, oxymethylene), 3.63−3.67 (m, 4H, oxymethylene), 3.76−3.78 (m, 4H, oxymethylene), 4.42−4.45 (m, 4H, oxymethylene), and 6.58 (s, 2H, quinone); IR (KBr) 2924, 1656, 1590, 1459, 1295, 1109, 1074, and 843 cm^{-1}; FAB-MS m/z 345 (M + 1), calcd for C$_{16}$H$_{24}$O$_8$, 344. Anal. Calcd for C$_{16}$H$_{24}$O$_8$: C, 55.81; H, 7.02. Found: C, 55.79; H, 7.11. UV/vis (CHCl$_3$): $\lambda_{max}(\epsilon)$ = 271 (2880) and 398 (1010) nm.

2,3-Bis(2′-(2″-(2‴-methoxyethoxy)ethoxy)ethoxy)-quinone (2c). Sodium hydroxide (8.0 g, 200 mmol) was added to a stirred solution of 3-benzyloxypyrocatechol, **9** (5.0 g, 23 mmol), and triethyleneglycol monomethyl ether tosylate, **6c** (14.6 g, 46 mmol), in dry dioxane (200 mL), and then the solution was heated at 80 °C for 24 h. The precipitate was filtered off, and the filtrate was evaporated under the reduced pressure to give a viscous residue. The residue was extracted with benzene to give 2,3-bis(2′-(2″-(2‴-methoxyethoxy)ethoxy)ethoxy)-1-benzyloxybenzene, **10c** (10.3 g, 88%). Subsequently, a mixture of **10c** and Pd carbon (1 g) in dioxane (10 mL) was stirred under an atmosphere of hydrogen for 3 days. The catalyst was filtered off, and the solvent was evaporated under the reduced pressure to give 2,3-bis(2′-(2″-(2‴-

methoxyethoxy)ethoxy)ethoxy)phenol, **11c** (7.9 g, 89%), as an oil. Fremy's salt (3.8 g, 14 mmol) was added to a stirred suspension of **11c** (1.3 g, 3 mmol) in 5% aqueous sodium acetate (280 mL) containing a small amount of benzene (30 mL). After the mixture had been stirred at room temperature for 30 min, it was extracted with benzene (3 × 70 mL). The combined organic layers were dried (MgSO$_4$) and concentrated under reduced pressure. The residue was chromatographed on a silica gel with chloroform−THF (14:1). After removal of solvent, **2c** was obtained as a red oil (0.46 g, 37%). **2c**: ^{1}H NMR (270 MHz) CDCl$_3$ δ 3.37 (s, 6H, Me), 3.51−3.55 (m, 4H, oxymethylene), 3.60−3.69 (m, 12H, oxymethylene), 3.75−3.79 (m, 4H, oxymethylene),

4.41−4.44 (m, 4H, oxymethylene), and 6.58 (s, 2H, quinone); IR (KBr) 2878, 1656, 1589, 1459, 1294, 1106, and 845 cm^{-1}; FAB-MS m/z 433 (M + 1), calcd for C$_{20}$H$_{32}$O$_{10}$, 432. Anal. Calcd for C$_{20}$H$_{32}$O$_{10}$: C, 55.55; H, 7.46. Found: C, 55.29; H, 7.66. UV/vis (CHCl$_3$): $\lambda_{max}(\epsilon) = 271$ (2460) and 400 (1020) nm.

Supporting Information Available: NMR spectra (PDF). This material is available free of charge via the Internet at http://pubs.acs.org.

JA021444T